Characterization of 2-((4-(chloromethyl)benzoyl)oxy)benzoate acid for analgesic tablet dosage form formulation

by Wuryanto Hadinugroho

Submission date: 20-Feb-2025 09:06PM (UTC+0700)
Submission ID: 2593758741
File name: 9-Characterization_of_2.pdf (3.69M)
Word count: 7947
Character count: 40874

Current Research in Pharmacology and Drug Discovery 7 (2024) 100200

Contents lists available at ScienceDirect

Current Research in Pharmacology and Drug Discovery

journal homepage: www.journals.elsevier.com/current-research-in-pharmacology-and-drug-discovery

Characterization of 2-((4-(chloromethyl)benzoyl)oxy)benzoate acid for analgesic tablet dosage form formulation

Wuryanto Hadinugroho *, Yudy Tjahjono, Kuncoro Foe, Senny Yesery Esar, Caroline Caroline, Maria Annabella Jessica, Hendy Wijaya

Faculty of Pharmacy, Widya Mandala Surabaya Catholic University, Surabaya, 60112, Indonesia

ARTICLE INFO

Keywords:
$4CH_2Cl$
Tablet
Formulation
Analgesic
Simplex lattice design

ABSTRACT

The 2-((4-(chloromethyl)benzoyl)oxy)benzoic acid ($4CH_2Cl$) is a potential analgesic compound derived from salicylic acid and 4-chloromethyl benzoyl chloride. Characterization required $4CH_2Cl$ for the formulation of tablet dosage forms. This study aims investigate the effect of SSG, PVP-K30, and the combination of SSG*PVP K-30 on the formulation of $4CH_2Cl$ tablets. Additionally, this study aimed to obtain the optimum $4CH_2Cl$ tablet composition. The experiment followed the two-factor simplex lattice design and direct compression method. The analgesic activity of $4CH_2Cl$ in the optimal tablet was investigated using the hot-plate methods. The ANOVA of linear models is acceptable and the polynomial coefficients of quadratic models are similar to those of linear models. The coefficient of the linear model shows that SSG and PVP K-30 increase the Carr index (16.26; 20.61), Hausner ratio (1.19; 1.29), hardness (4.19; 9.39), friability (0.48; 0.67), disintegration time (0.34; 7.50), and drug release (85.29; 97.69). The coefficient of the quadratic model shows that SSG*PVP K-30 increased the Carr index (1.90), Hausner ratio (0.04), hardness (1.88), friability (0.06), and drug release (4.56), and decreased disintegration time (−0.30). SSG and PVP K-30 increased Carr index, Hausner ratio, hardness, friability, disintegration time, and drug release. The combination of SSG*PVP K-30 has the same effect, except that the disintegration time decreased. The optimum tablet formula is $4CH_2Cl$ (300 mg), Ne (75 mg), SSG (33.60 mg), PVP K-30 (22.40 mg), MCC (40 mg), and SDL (up to 800 mg). $4CH_2Cl$ tablets can be a candidate and choice for new analgesic drugs in the future.

1. Introduction

$4CH_2Cl$ is a salicylic acid derivative originating from salicylic acid and 4-chloromethyl benzoyl chloride. $4CH_2Cl$ has analgesic potential and relatively low gastric ulceration side effects [Sugiarno, 2016; Tamayanti et al., 2016]. Tablets are the best choice for obtaining the solid $4CH_2Cl$ compound with an exact measurable dosage and relatively simple administration (mainly orally). Caroline and colleagues have reported the Pharmacokinetic parameters of this compound, namely: maximum concentration in blood plasma (C_{max} 0.53 μg/mL), time to reach maximum concentration in blood plasma (t_{max} 16.91 min), elimination rate (K_{el}. 0.02 min^{-1}), time is eliminated in half ($t_{1/2}$ el. 41.72), and partition coefficient (log P 3.73). The $4CH_2Cl$ powder is white and forms aggregates when stored at ambient temperature (Sugiarno, 2016; Tamayanti et al., 2016).

The novelty of this study is in characterizing and formulating $4CH_2Cl$ as a new analgesic compound in tablet dosage form using excipients that match the characteristics of the $4CH_2Cl$. The crucial excipients are insulators, disintegrants, and solubilizers. Neusilin (Ne) is insulating agent is used to prevent $4CH_2Cl$ particle aggregation. Sodium starch glycolate (SSG) is a disintegrant that increases the tablet's ability to disintegrate into granules or powders, supporting the dissolution process during oral administration. SSG is a relatively affordable and easily obtained disintegrating agent. Additionally, SSG particles are round, and the surface morphology is smooth (Hadinugroho et al., 2022b; Sheskey et al., 2017)]. These characteristics are very supportive for making tablets by direct compression. The action of SSG involves particles swelling when hydrated, thereby pushing the surrounding particles to separate from each other (Hadinugroho et al., 2022b; Markl and Zeitler, 2017). PVP K-30 is a solubilizer that increases the solubility of $4CH_2Cl$ by reducing the difference in polarity between the media and $4CH_2Cl$ particles, thus reducing the lipophilicity of $4CH_2Cl$. A low concentration of PVP K-30

* Corresponding author.
E-mail address: wuryanto.hadinugroho@ymail.com (W. Hadinugroho).

https://doi.org/10.1016/j.crphar.2024.100200
Received 8 October 2023; Received in revised form 1 August 2024; Accepted 2 September 2024
Available online 7 September 2024

significantly increases the solubility of $4CH_2Cl$. PVP K-30 is easily soluble and forms a gel before dissolving. PVP K-30 particles have a smooth surface morphology, supporting the manufacture of tablets by direct compression. Additionally, PVP K-30 is a potent solubilizer, making it effective and efficient (Kurakula and Rao, 2020; Sheskey et al., 2017). In general, the current manuscript presents an adjustment on the formula from previous studies on 2-((3-(chloromethyl)benzoyl)oxy)benzoic acid ($3CH_2Cl$) tablets, using tablet excipients with characteristics adjusted to $4CH_2Cl$ to make it more effective and efficient (Hadinugroho et al., 2022a; Hadinugroho et al., 2022a), Based on the yield synthesis experiment, $4CH_2Cl$ is more abundant than $3CH_2Cl$, which suggests that $4CH_2Cl$ could be more economical for mass production in tablet dosage form.

This study aimed to investigate the effect of SSG, PVP-K30, and the combination of SSG*PVP K-30 on the formulation of $4CH_2Cl$ tablets. Additionally, this study aimed to obtain the optimum $4CH_2Cl$ tablet composition. The experiment followed a two-factor simplex lattice design. The optimization factors are the concentration of SSG and PVP K-30. The optimization responses are the Carr index, Hausner ratio, hardness, friability, disintegrating time, and drug release. The optimization response and the optimum formula are analyzed using optimization software. The optimum tablet was used to test analgesic activity with a hot plate. This study can provide a new choice of analgesic tablets.

2. Material and methods

2.1. Raw materials and chemicals

The quality of the materials used in this study was analytical grade (p.a), pharmaceutical grade (p.g), and food grade (f.g). Salicylic acid (p.g.) (PT. Brataco, Indonesia), 4-chloromethyl benzoyl chloride (p.a.) (Sigma-Aldrich, GmbH, USA), pyridine (p.a.) (Merck KgaA, Darmstadt, Germany), neusilin (p.g.) (Gangwal Chemicals, India), sodium starch glycolate (p.g.) (JRS Pharma, India), polyvinyl pyrrolidone K-30 (BASF Corp., Germany), microcrystalline cellulose (p.g.) (Flocel 102, Gujarat Microwax PVT. LTD, India), spray-dried lactose (p.g.) (Foremost Farm, USA), sodium hydroxide (p.a.) (Merck KgaA, Darmstadt, Germany), potassium dihydrogen phosphate (p.a.) (Merck KgaA, Darmstadt, Germany), ethanol (p.a.) (Merck KgaA, Darmstadt, Germany), and distilled water (f.g.) (Brataco Chemical, Indonesia).

2.2. Synthesis of $4CH_2Cl$

The synthesis of $4CH_2Cl$ adopts the previously described methods (Caroline et al., 2019b; Hadinugroho et al., 2022a; Tjahjono et al., 2021). Salicylic acid (1.8 mmol) and 4-chloromethyl benzoyl chloride (7.2 mmol) were mixed in an Erlenmeyer flask. Pyridine (1.7×10^{-6} mmol) and acetone (14.8×10^{-6} mmol) were added to form a wet mass of $4CH_2Cl$. This mixture was then irradiated with microwaves for 5 min using a Millstone Organic Synthesis Unit (MicroSYNTH) to produce solid $4CH_2Cl$. Unreacted salicylic acid was identified using ferric chloride ($FeCl_3$) and precipitated with ethanol-water to separate and purify the $4CH_2Cl$ compound. The $4CH_2Cl$ was characterized by Fourier transform infrared (FTIR), nuclear magnetic resonance (NMR), thin-layer chromatography (TLC), UV spectrophotometry, and melting point analysis.

2.3. Fourier transform infrared spectroscopy

The structure of $4CH_2Cl$ was analyzed by Fourier transform infrared spectroscopy (UATR PerkinElmer Spectrum Version 10.4.3), and recorded at a wave number of 4000-450 cm^{-1}.

2.4. Nuclear magnetic resonance

^{1}H and ^{13}C NMR of $4CH_2Cl$ was analyzed by liquid state NMR spectroscopy (JEOL RESONANCE 500 MHz, Japan) with acetone as solvent.

2.5. Thin layer chromatography

The $4CH_2Cl$ (50 mg) was dissolved in ethanol (50 mL) and spotted (5 μL) on a 60 F254 silica gel plate (Merck, Germany) as the stationary phase. The plate was eluted in the chamber containing the saturated mobile phase. The mobile phase (v/v) used was ethyl acetate: ethanol (2:1); n-hexane: ethanol (1:2); and chloroform: methanol (4:1). The dry plate was observed with a UV lamp at 254 nm to determine the spot and the retention value (Rf). SA and 4-chloromethyl benzoyl chloride were used as a comparison.

2.6. Spectrophotometer

The wavelength of $4CH_2Cl$ by spectrophotometer determined the $4CH_2Cl$. A solution of $4CH_2Cl$ in ethanol (20 g/mL) was observed with a UV–VIS spectrophotometer (Hitachi U-1100, Jepang) at 200–400 nm and determined the maximum wavelength.

2.7. Melting point

The melting point of $4CH_2Cl$ was determined using an Optimelt MPA 100 apparatus (USA). The temperature was set from 140 °C to 170 °C at a rate of 1 °C per minute. Approximately 2 mm of $4CH_2Cl$ powder was placed in a capillary tube, which was then inserted into the melting point apparatus, and the melting point was recorded.

2.8. Tablet manufacturing

The tablet formulation contained $4CH_2Cl$ (300 mg), Ne (75 mg), MCC (40 mg), and SDL (up to 800 mg). Table 1 presents the PVP K-30 and SSG quantities, with a production capacity of 120 g tablet mass or 150 tablets. $4CH_2Cl$ and Ne were mixed homogeneously in a mortar and pestle. The other ingredients (SSG, PVP K-30, MCC, and SDLwere added and blended in a cubic mixer (Erweka, Germany) at 100 rpm for 2 min. The mixture's compressibility was assessed, and the tablet mass was compressed into 800 mg tablets using a single-punch tablet press (Jenn Chian Machinery, Taiwan). The tablets were evaluated for hardness, friability, and disintegration time. A dissolution test was conducted to determine drug release.

The selection of the dose of $4CH_2Cl$ 300 mg per tablet follows the dose of $3CH_2Cl$ tablets, which is a salicylate derivative that has been reported previously in previous experiments (Hadinugroho et al., 2022a). Pharmacokinetic data of C_{max} and K_{el} in rats show similarities between $4CH_2Cl$ and $3CH_2Cl$. $4CH_2Cl$ has a C_{max} of 0.53 μg/mL and K_{el} of 0.020 min^{-1}, while $3CH_2Cl$ has a C_{max} of 0.57 μg/mL and K_{el} of 0.018 min^{-1} (Caroline et al., 2019a; Sugiarno, 2016). Dose calculations were also performed and presented in the supplementary material Chapter S1.

2.9. Compressibility

Tablet mass was placed in a known-weight 100 mL measuring tube, and the initial weight was recorded. The tube was placed on a tapped

Table 1
The detailed composition of each formula.

Material	Ta	Tb	Tc	To
$4CH_2Cl$ [mg]	300.00	300.00	300.00	300.00
Ne [mg]	75.00	75.00	75.00	75.00
MCC [mg]	40.00	40.00	40.00	40.00
SSG [mg]	40.00	32.00	24.00	33.60
PVP K-30 [mg]	16.00	24.00	32.00	22.40
SDL [mg]	329.00	329.00	329.00	329.00

density volumeter (Erweka, Germany) and tapped 500 times. Volumes before and after tapping were recorded to calculate bulk density (Bd) and tapped density (Td). The Carr index and Hausner ratio were calculated using Equations (1) and (2), respectively (Aulton and Taylor, 2017; Hadinugroho et al., 2022b).

$$Carr\ index\ [\%] = \frac{Td - Bd}{Td}\ x\ 100\% \qquad \text{Equation 1}$$

$$Hausner\ ratio = \frac{Td}{Bd}\ x\ 100\% \qquad \text{Equation 2}$$

2.10. Hardness

Hardness was tested on six randomly selected tablets using an hardness tester (Erweka, Germany). Tablets were horizontally pressed with a metal block until they cracked, and the hardness was displayed on the apparatus monitor (Aulton and Taylor, 2017; The United States Pharmacopeial Convention, 2018).

2.11. Friability

Several tablets (10) were taken randomly because the weight per tablet was more than 650 mg or the total weight of 10 tablets was more than 6500 mg. Each tablet was dust-free, and selected tablets were weighed (W). All tablets were placed and rotated on a drum friability tester (Erweka, Germany) (25 rpm, 4 min). Each tablet was dust-free again and weighed (W'). Friability is determined according to Equation (3) (Aulton and Taylor, 2017; The United States Pharmacopeial Convention, 2018).

$$friability\ [\%] = \frac{W - W'}{W}\ 100\% \qquad \text{Equation 3}$$

2.12. Disintegration time

Six tablets were randomly selected from 18 tablets (Aulton and Taylor, 2017; The United States Pharmacopeial Convention, 2018). The tablets were placed in each holder of the disintegration tester (Erweka Z3, Germany). The tube moves reversibly vertically in the distilled water medium chamber (37 °C; 900 mL). The longest time, where the tablets disintegrated completely from 6 tablets in the holder, is defined as the disintegration time.

2.13. Dissolution

The tablets were dissolved using 900 mL of phosphate buffer medium pH 6.8 (37 ± 0.5 °C; 50 rpm). The test was carried out using the basket method for 60 min (Bertocchi et al., 2005; Hadinugroho et al., 2022a; The United States Pharmacopeial Convention, 2018; Zupančič-Božič et al., 1997). The concentration of dissolved $4CH_2Cl$ was determined by UV–VIS spectrophotometer (Hitachi U-1900, Japan) with a wavelength of about 242 nm.

2.14. Optimization of $4CH_2Cl$ tablets

The optimization method used is a two-factor simplex lattice. We investigated the optimal concentration of SSG (24–40 mg) and PVP K-30 (16–32 mg). The optimization responses are the Carr index, Hausner ratio, hardness, friability, disintegrating time, and drug release. Preliminary experiments with a comparison of SSG (mg) and PVP K-30 (mg) were Ta (40:16), Tb (32:24), and Tc (24:32). Response processing using optimization software (Design Expert ver 10) and statistical analysis using ANOVA linear and quadratic model approaches (Hadinugroho et al., 2022a).

2.15. Release kinetics of $4CH_2Cl$ from tablets

The release kinetics of $4CH_2Cl$ tablets from three formulas were analyzed by DDSolver software. The release kinetics model used is Higuchi, Korsmeyer-Peppas, and first order (Equations (4)–(7)) (Craciun et al., 2019; Kaleemullah et al., 2017; Panotopoulos and Haidar, 2018; Wahab et al., 2011):

$$\text{First order} \quad : \ln C_t = \ln C_o + K_o.t \qquad \text{Equation 4}$$

Ct: drug dissolved at time [g], Co: initial drug [g], and Ko: constant drug release [h^{-1}].

$$\text{Higuchi} \quad : C_t = K_H.\sqrt{t} \qquad \text{Equation 5}$$

Ct: drug dissolved at time [g], K_H: Higuchi constant [$g/h^{1/2}$], and t: time [h].

$$\text{Korsmeyer} - \text{Peppas} \quad : C_t/C_\infty = K_K.\ t^n \qquad \text{Equation 6}$$

C_t/C_∞: released drug fraction [g], K_k: Korsmeyer-Peppas constant [g.h], and n: diffusion exponential.

$$\text{Weibull} \quad : \log[\ln - (1 - m)] = b\log(t - Ti) - \log a \qquad \text{Equation 7}$$

(1-m): insoluble drug portion [g], Ti: lag time before dissolution, a: initial drug [g], b: parameter of curve slope.

2.16. Animal models and analgesic activity

Nine male BALB/C mice (1–2 months old; 20–25 g) were sourced from the Pharma-Veterinary Center of Surabaya, Indonesia. The mice were kept in a room with controlled temperature (20–24 °C) and 65% relative humidity, on a 12-h light/dark cycle. They were acclimatized for 7 days before the study began. All animal procedures followed Institutional Animal Care and Use Committee (IACUC) guidelines and received ethical approval by preclinical ethic committee Faculty of Veterinary Sciences, Gadjah Mada University, Yogyakarta-Indonesia No. 001/ECFKH/Eks/2022. The mice had free access to food and water throughout the 24-day period, including the acclimatization phase, with temperature recorded twice daily. The mice were assigned to three groups (n = 3 per group): control (untreated), ASA (Comparison), and $4CH_2Cl$ ("To" group). ASA (Bayer, Leverkusen, Germany) or $4CH_2Cl$ was given orally at a single dose of 60 mg/kg B, based on previously published methods (Tjahjono et al., 2024). The untreated groups were given 3% Pulvis Gummi Arabicum as a placebo. Analgesic activity experiment using the writhing test method. Pain induction was created by intraperitoneal injection of 0.6% acetic acid (0.01 mL/g body weight), according to previously published methods (Caroline et al., 2019a; Tjahjono et al., 2021). The successful induction response of pain induction was demonstrated by the mice writhing, which was observed for 10 min.

3. Result

3.1. $4CH_2Cl$ synthesis reaction mechanism

$4CH_2Cl$ synthesis reaction mechanism are presented in Fig. 1. The reaction begins with the attack of pyridine on Cl on 4-chloromethyl benzoyl chloride. Cl^- is released and pyridine binds to 4-chloromethyl benzoyl chloride **(a)**. The compound created is more electrophilic than 4-chloromethyl benzoyl chloride. OH on the phenolic of SA attacks the C atom at C=O of the compound and bonds to create a new compound **(b)**. The pyridine ion is released and bonds with Cl^-, called pyridine chloride. Simultaneously, the H atom at OH of the phenolic comes from SA is released so that the O atom loses an electron and bonds with the C atom at C=O of 4-chloromethyl benzoyl chloride, which loses an electron **(c)**. The O atom at C=O, which comes from 4-chloromethyl benzoyl

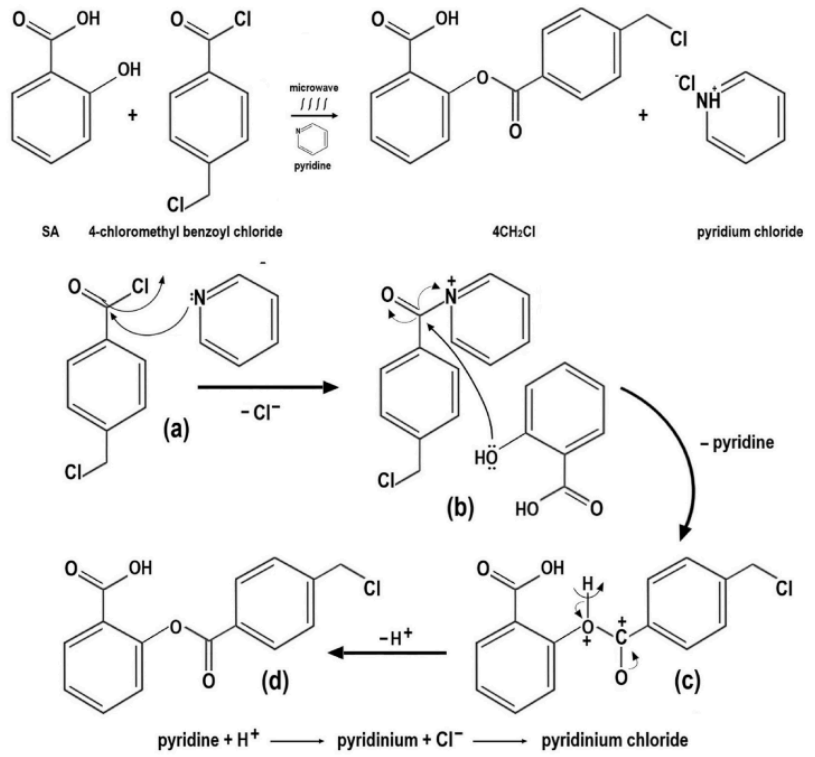

Fig. 1. 4CH2Cl synthesis reaction mechanism.

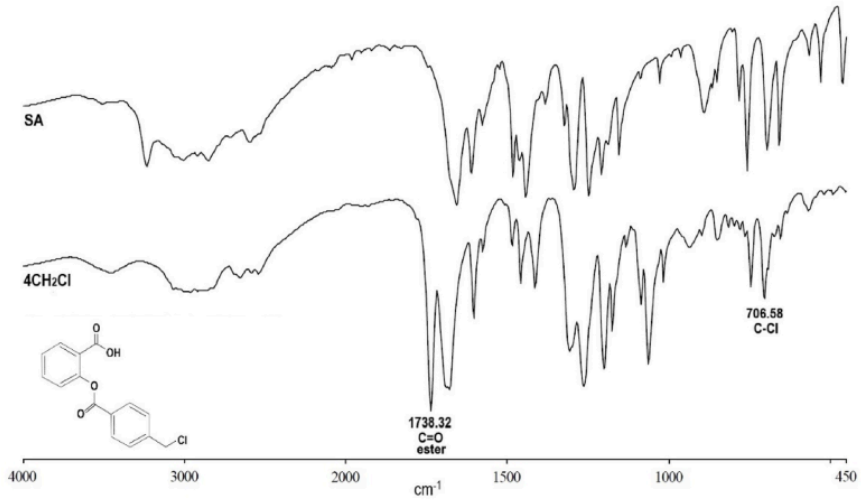

Fig. 2. FTIR spectrum of $4CH_2Cl$ and SA. The presence of the ester carbonyl group (C=O) and C-Cl in $4CH_2Cl$ is a specific group and is not present in SA.

chloride, gains an electron so that a double bond occurs and $4CH_2Cl$ is created **(d)**.

3.2. Fourier transform infrared spectroscopy

The infrared spectra of $4CH_2Cl$ and SA are shown in Fig. 2. The $4CH_2Cl$ spectra showed the carbonyl ester peak (C=O) appeared at a wavelength of 1738.32 cm^{-1} and the carboxylate peak (C=O) appeared at 1682.37 cm^{-1}. The peak of C-O appears at wavelengths 1309.45 cm^{-1}, 1264.38 cm^{-1}, and 1201.42 cm^{-1}. The peak of C-Cl appears at a wavelength of 706.58 cm^{-1}. The SA spectra showed the carboxylate peak (C=O) appeared at 1658.14 cm^{-1}. The peak of C-O appears at wavelengths 1295.17 cm^{-1}, 1249.16 cm^{-1}, and 1210.21 cm^{-1}

3.3. Nuclear magnetic resonance

The NMR analysis was performed as a follow-up infrared analysis to confirm the success of the synthesis. The NMR spectra of $4CH_2Cl$ are shown in Fig. 3. The ^1H NMR spectrum of $4CH_2Cl$ shows C-H peaks at δ = 8.145 ppm (14), δ = 8.078 ppm (1), δ = 7.565 ppm (5.10), and δ = 7.635 ppm (6)(11)(13). CH-Cl peaks at δ = 4821 ppm (15).

The ^{13}C NMR spectra of $4CH_2Cl$ show a carbonyl ester peak (C=O) at δ = 164.482 ppm (8); carboxylate peak (C=O) at δ = 165.026 ppm (7); C-Cl peak at δ = 45.157 ppm (15). C-H peak at δ = 151.96 ppm (3); δ = 143.592 ppm (11); δ = 133.934 ppm (5)(12); δ = 131.865 ppm (1); δ = 130,482 ppm (13); δ = 129.986 ppm (9); δ = 129.881 ppm (10); δ = 129.004 ppm (14); δ = 126.220 ppm (6); and δ = 124.132 ppm (2)(4).

3.4. Thin layer chromatography

The chromatograph of $4CH_2Cl$, SA, and 4-chloromethyl benzoyl chloride is shown in Fig. 4. The Rf value of $4CH_2Cl$ with ethyl acetate: ethanol (1:2) is 0.82(3)(4); n-hexane: ethanol (1:2) is 0.81 (3)(4); and chloroform: ethanol (4:1) is 0.86 (3)(4). The Rf value of SA with ethyl acetate: ethanol (1:2) is 0.80 (1); n-hexane: ethanol (1:2) is 0.72 (1); and chloroform: ethanol (4:1) is 0.69 (1). The Rf value of 4-chloromethyl benzoyl chloride with ethyl acetate: ethanol (1:2) is 0.95 (2); n-hexane: ethanol (1:2) is 0.90 (2); and chloroform: ethanol (4:1) is 0.98 (2).

3.5. Spectrophotometer

The UV spectra of $4CH_2Cl$ are shown in Fig. 5. Screening the

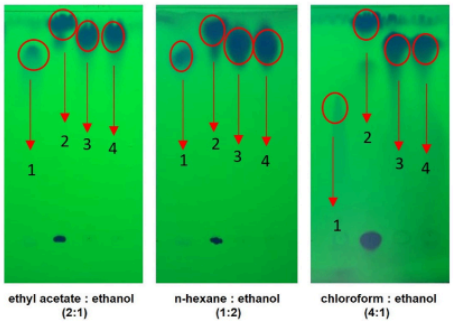

Fig. 4. Chromatogram of thin layer chromatography with multiple mobile phases. Spot 1 is SA, spot 2 is 4-chloromethyl, and spot 3, 4 is $4CH_2Cl$.

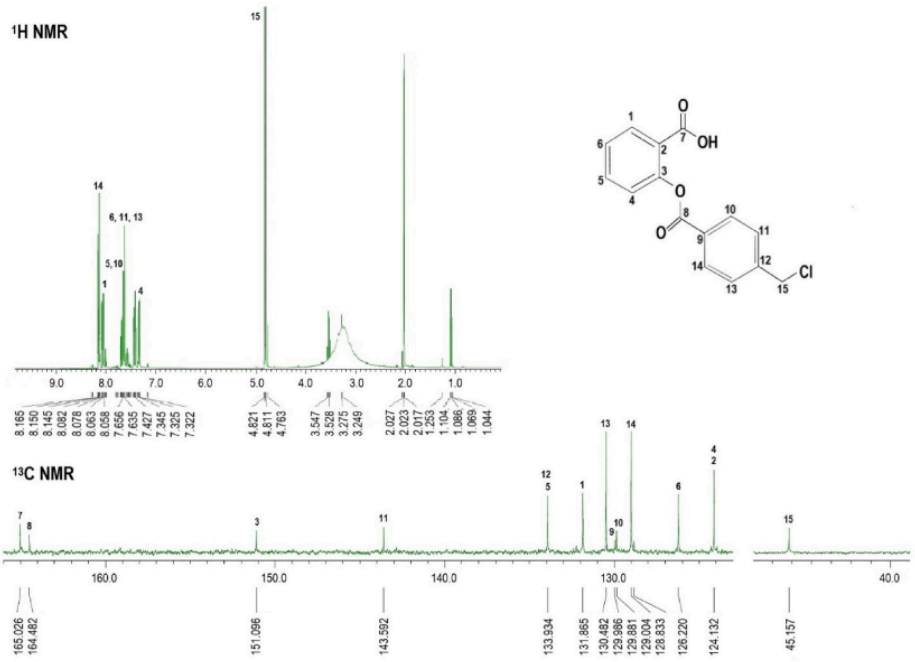

Fig. 3. ^1H and ^{13}C NMR spectrum of $4CH_2Cl$. The presence of carbonyl ester group (C=O) (δ = 164.482 ppm) and C-Cl (δ = 45.157 ppm) are specific groups.

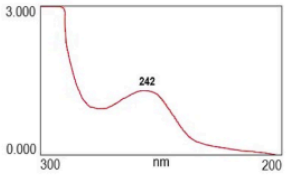

Fig. 5. UV spectra of $4CH_2Cl$. The maximum wavelength of $4CH_2Cl$ is at 242 nm.

maximum wavelength of the $4CH_2Cl$ peak is about 242 nm. The maximum wavelength of SA is about 212 nm. The difference in maximum wavelength shows that the chemical structure of $4CH_2Cl$ is different from that of SA.

3.6. Melting point

The melting point of $4CH_2Cl$ is 157–159 °C. It is similar to the melting point of SA (158–160 °C).

3.7. Compressibility of 4CH2Cl tablets mass

Compressibility is determined as the ratio between the Carr index and the Hausner ratio. The values of each parameter for the three produced tablet masses are shown in Table 2. The value of the quadratic polynomial coefficient of the Carr index and Hausner ratio are PVP K-30 (20.45) (1.29), SSG (16.10) (1.19), and SSG*PVP K-30 (1.90) (0.04). The ANOVA results from the Carr index and Hausner ratio of linear models are acceptable, and the polynomial coefficients of quadratic models are similar to those of linear models (Table 2).

3.8. The hardness of $4CH_2Cl$ tablets

The hardness of $4CH_2Cl$ tablets is presented in Table 2. The hardness of Tc tablets is higher than that of Ta and Tb tablets. Tablet hardness occurs due to the interlocking between the particles of the tablet mass. The value of the quadratic polynomial coefficient of PVP K-30 (9.23), SSG (4.03), and SSG*PVP K-30 (1.88). The ANOVA results from the hardness of linear models are acceptable, and the polynomial coefficients of quadratic models are similar to those of linear models (Table 2).

3.9. Friability of $4CH_2Cl$ tablets

The friability is presented in Table 2. The most friable tablets are Tc, Tb, and Ta tablets. The value of the quadratic polynomial coefficient of PVP K-30 (0.66), SSG (0.47), and SSG*PVP K-30 (0.06). The friability ANOVA of the linear model was accepted, and the polynomial coefficients of quadratic models are similar to those of linear models (Table 2).

3.10. Disintegration time of $4CH_2Cl$ tablets

The disintegration time of $4CH_2Cl$ tablets is presented in Table 2. The value of the quadratic polynomial coefficient of PVP K-30 (7.75), SSG (0.59), and SSG*PVP K-30 (−0.30). The disintegration time ANOVA of the linear model was accepted, and the polynomial coefficients were similar to that of the quadratic model (Table 2).

3.11. Dissolution of $4CH_2Cl$ tablets

The release and dissolution profiles of $4CH_2Cl$ are presented in Table 2 and Fig. 6. Dissolution data processing uses a standard curve for phosphate buffer pH 6.8 with equation $Y = 0.1384 + 0.0714.X$. The order of tablets with the highest release of $4CH_2Cl$ was Tc, Tb, and Ta. The value of the quadratic polynomial coefficient of PVP K-30 (97.31), SSG (84.91), and SSG*PVP K-30 (4.56). The drug release ANOVA of the linear model was accepted, and the polynomial coefficients were similar to the quadratic model (Table 3).

3.12. Optimization of $4CH_2Cl$ tablets

The experimental design followed a 2-factor simplex lattice (SSG and PVP K-30). The linear and quadratic statistical model predicts the effects of SSG, PVP K-30, and SSG*PVP K-30 (Table 3 and Supplementary Material Table S1). The ANOVA evaluated the acceptability of the linear model by considering the values of R-Squared, Adj R-Squared, Pred R-Squared, and Adeq Precision. The linear model is accepted if the R-Square and Pred R-Square have a difference of less than 0.2, Adeq Precision of more than 4, and R-Square is close to one. All optimization response parameters meet the specifications so that the coefficients are accepted. The coefficient quadratic model profile is similar to the linear model so that the combined coefficient of the two can be used to predict

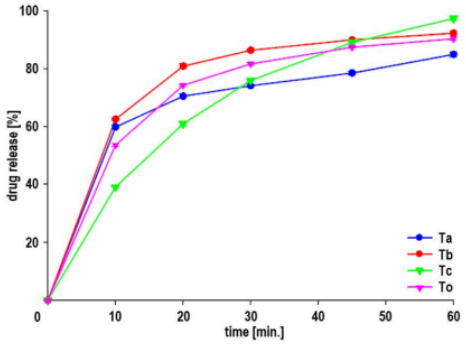

Fig. 6. The dissolution profile of Ta, Tb, Tc, and To tablets. The compositions of SSG [mg] and PVP K-30 [mg] are Ta (40.00 : 16.00), Tb (32.00 : 24.00), Tc (24.00 : 32.00), and To (33.60 : 22.40).

Table 2
Detail evaluate of tablets mass, tablets, and dissolution of $4CH_2Cl$.

Tablet	SSG	PVP K-30	Carr index		Hausner ratio		Hardness		Friability		Disintegrating time		Drug release	
Code	[mg]	[mg]	[%]	SD		SD	[kp]	SD	[%]	SD	[min.]	SD	[%]	SD
Ta	40.00	16.00	16.10	0.13	1.19	0.01	4.03	0.04	0.47	0.10	0.59	0.10	84.91	0.92
Tb	32.00	24.00	18.75	0.28	1.25	0.01	7.10	0.07	0.57	0.11	1.37	0.09	92.25	0.53
Tc	24.00	32.00	20.45	0.23	1.29	0.01	9.23	0.14	0.66	0.12	7.75	0.13	97.31	0.66
Tp	33.60	22.40	18.00	–	1.24	–	6.56	–	0.55	–	3.20	–	90.25	–
To	33.60	22.40	18.10	0.10	1.24	0.02	6.51	0.22	0.54	0.14	3.30	0.16	90.30	0.54

Tp (prediction tablet): composition and quality prediction follow software design expert.
To (optimum tablet): the composition follows the software design expert, and the quality value is the result of the verification experiment.

Table 3
Statistic of tablets mass, tablets, and dissolution of $4CH_2Cl$.

Parameter	ANOVA				Polynomial		To
	R-Squared	Adj R-Squared	Pred R-Squared	Adeq Precision	linier	quadratic	t
Carr index	0.9844	0.9687	0.7887	13.7368	*Y = 16.26 A + 20.61 B*	*Y = 16.10 A + 20.45 B + 1.90 A*B*	1.732
Hausner ratio	0.9868	0.9737	0.8224	15.0000	*Y = 1.19 A + 1.29 B*	*Y = 1.19 A + 1.29 B + 0.04 A*B*	0.378
Hardness	0.9892	0.9784	0.8545	16.5957	*Y = 4.19 A + 9.39 B*	*Y = 4.03 A + 9.23 B + 1.88 A*B*	0.388
Friability	0.9918	0.9835	0.8887	19.0000	*Y = 0.48 A + 0.67 B*	*Y = 0.47 A + 0.66 B + 0.06 A*B*	0.085
Disintegrating time	0.9856	0.9712	0.8053	14.3200	*Y = 0.34 A + 7.50 B*	*Y = 0.59 A + 7.75 B - 0.30 A*B*	1.076
Drug release	0.9889	0.9777	0.8496	16.3158	*Y = 85.29 A + 97.69 B*	*Y = 84.91 A + 97.31 B + 4.56 A*B*	0.172

the effect of SSG*PVP K-30. The optimum tablet (To) was determined according to a numerical linear model. The prediction of the optimum tablet composition (Tp) and the verification results are presented in Table 3.

3.13. The release model kinetics of $4CH_2Cl$ from tablets

The analysis of the release $4CH_2Cl$ was performed using DDSolver as shown in Table 3 and Fig. 7 (for details, see Supplementary Material in Figs. S1–S4). The analysis parameters are Rsqr_adj, MSE_root, and Akaike Information Criterion (AIC).

3.14. $4CH_2Cl$ tablet inhibits acetic acid induced pain in mice

Both $4CH_2Cl$ (32.22 ± 2.25 s response time) and ASA groups (52.83 ± 3.87 s response time) showed reduced writhing frequency ($P < 0.05$) when compared with the placebo group (78.33 ± 4.16 s response time). The $4CH_2Cl$ test group also gave less writhing frequency than the ASA group ($p = 0.05$) (Fig. 8).

4. Discussion

The success of the synthesis was chemically confirmed using infrared and magnetic resonance. The infrared spectra showed the specific peak $4CH_2Cl$ that SA did not have was C=O and C-Cl (Coates, 2006). The specific peak ^{13}C NMR of $4CH_2Cl$ show a carbonyl ester peak (C=O) at δ = 164.482 ppm and C-Cl peak at δ = 45.157 ppm (Flemming, 2016; Kupriyanova et al., 2021). On the chromatogram, the difference in the Rf value of $4CH_2Cl$ with SA and 4-chloromethyl benzoyl chloride indicates a change in chemical structure, resulting in a change in the compound's polarity. The Rf value for each mobile phase can provide information on the polarity of $4CH_2Cl$ to support the formulation of pharmaceutical preparations. The spectrophotometer wavelength of $4CH_2Cl$ is longer than SA because $4CH_2Cl$ contains two benzene chromophores that can

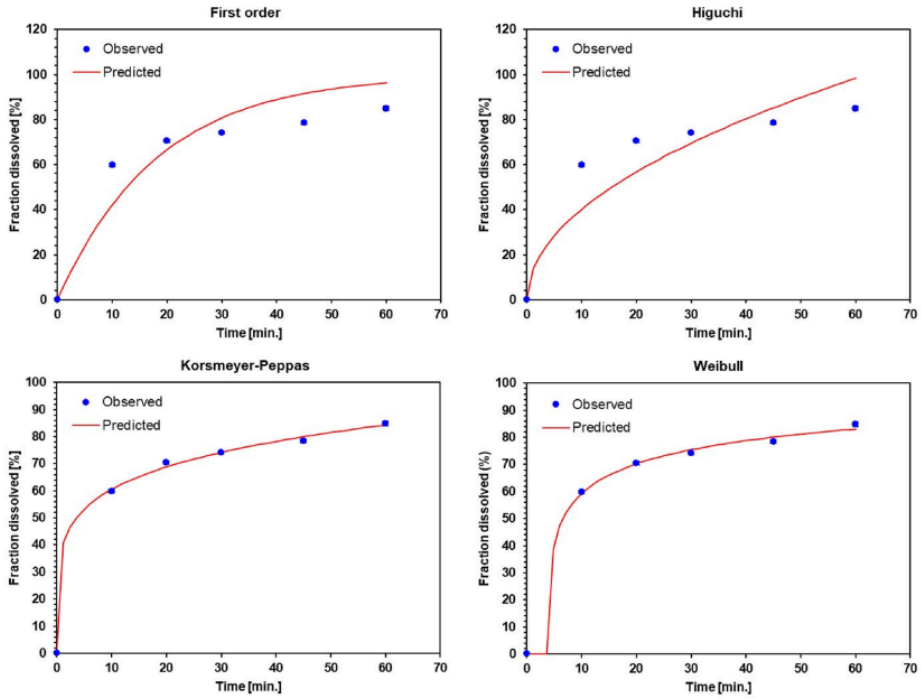

Fig. 7. Release kinetics model of $4CH_2Cl$ from Ta, Tb, Tc, and To tablets. The compositions of SSG [mg] and PVP K-30 [mg] are Ta (40.00 : 16.00) (Korsmeyer-Peppas), Tb (32.00 : 24.00) (Weibull), Tc (24.00 : 32.00) (First order, and To (33.60 : 22.40) (Weibull).

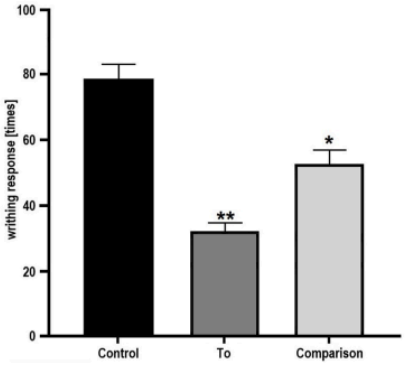

Fig. 8. Analgesic activity of $4CH_2Cl$. Placebo are mices given tablets containing excipients as control. ASA are mices given ASA tablets as a comparison. $4CH_2Cl$ are mices given $4CH_2Cl$ tablets (To).

absorb UV light (Dachriyanus, 2004; Suhartati, 2017). This wavelength provides a reference for quantitative analysis of $4CH_2Cl$ concentrations in various pharmaceutical dosage forms. The value of melting point indicates that $4CH_2Cl$ is relatively stable at ambient temperature, around 25°C. In addition, the melting point is considered in determining the method of preparing pharmaceutical dosage forms.

The $4CH_2Cl$ tablets contain Ne, SSG, PVP K-30, MCC, and SDL. Ne acts as an insulator between the $4CH_2Cl$ particles so that the particles do not aggregate together. The hydrophobicity of Ne in $4CH_2Cl$ improves the flow properties that support the tablet manufacturing process (Juneja et al., 2014; Lou et al., 2013; Shete et al., 2019). SSG acts as a disintegrating agent, accelerating the tablet disintegration. The SSG particles swell when hydrated, so the SSG particles push against the surrounding particles, and the tablet disintegrates (Hadinugroho et al., 2022b; Markl and Zeitler, 2017; Sheskey et al., 2017). PVP K-30, as a solubilizer, accelerates tablet hydration in the disintegration and dissolution processes (Kurakula and Rao, 2020; Sheskey et al., 2017). PVP K-30 accelerates SSG particles' hydration, so the tablet disintegrates quickly. In addition, PVP K-30 accelerates the solubility of $4CH_2Cl$ particles, thereby increasing the concentration of dissolving $4CH_2Cl$. MCC is used as a tablet filler because MCC has good compactibility. SDL is a filler because SDL has high density and good compactibility (Chaerunisaa et al., 2020; Thoorens et al., 2014; Yasmin et al., 2020). The combination of MCC and SDL can produce tablets with proportional thickness and diameter.

Analysis of tablet mass (Ta, Tb, and Tc) yielded a Carr index value between 16 until 20% and a Hausner ratio of less than 1.25 (Aulton and Taylor, 2017). This value means that the three tablet masses are good enough to flow, and the particle arrangement is quickly stable when subjected to mechanical forces. The tablet mass can move freely and fill the tablet machine die so that the tablet weight is achieved and consistent. Based on the value of the quadratic polynomial coefficient, the most influential parameter on the Carr index and Hausner ratio are PVP K-30, SSG, and SSG*PVP K-30. PVP K-30 particles are rounded and hollow and have a flat surface. The hollow PVP K-30 particles break easily to form fragments when subjected to mechanical movement, so the tablet mass requires a lot of activity to achieve a compressed particle arrangement. SSG particles are rounded and have a flat surface. The variation of the rounded shape involves a lot of mechanical movement for the arrangement of the tablet mass particles to become a compress. The lowest combination of SSG*PVP K-30 increases the Carr-index and Hausner ratio because PVP K-30 fragments can fill the porosity of the tablet mass so that a little mechanical movement can form a compressed tablet mass arrangement. Rounded shape with a flat surface of both particles, the tablet mass has good flow properties.

The tablet hardness specifications in this experiment were 4–8 kp. The materials that increase tablet hardness the most are PVP K-30, SSG, and SSG*PVP K-30. The PVP K-30 material has hygroscopic properties. When the tablet mass is compressed, the PVP K-30 particles become moist due to the heat of compression. The moisture derived from PVP K-30 particles can bind to the deformation of the tablet mass particles. When the tablet mass is compressed, the deformation of the SSG particles creates a narrow porosity in the interlocking deformation of the tablet mass particles. The lowest SSG*PVP K-30 increases tablet hardness. PVP K-30 fragment causes wide porosity in the interlocking deformation of tablet mass particles.

The tablet friability specifications in this experiment was ≤1% (The United States Pharmacopeial Convention, 2018). Tc tablets are more friable than Ta and Tb tablets. Tc tablets are the most friability but have the highest hardness. The friability occurs on the tablet's surface, releasing particles or fines. The interlocking particles on the tablet surface are removed when mechanical motion is applied. The materials that increased the tablet friability the most were PVP K-30, SSG, and SSG*PVP K-30. The PVP K-30 materials could raise the friability because the PVP K-30 fragments could not adhere firmly to the tablet surface. The variation in the rounded shape of SSG resulted in many interlocking porosity deformation particles on the tablet surface. The combination of SSG*PVP K-30 slightly increased tablet friability due to the strong interlocking of particle deformation on the tablet surface. The interlocking strength is obtained from the moisture of the PVP K-30 fragments when rubbing against each other produces heat so that the particles' deformation on the tablet's surface is not easily separated.

All tablets had a disintegration time of fewer than 30 min (The United States Pharmacopeial Convention, 2018). The SSG particles could swell when hydrated so that the surrounding tablet mass particles are pushed and separated from each other. The materials that increase the disintegration time the most are PVP K-30 and SSG. The combination of SSG*PVP K-30 reduces the disintegration time. The PVP K-30 dominates the increase in disintegration time because the PVP K-30 particles are hydrated to form a viscous gel to bind the particles, and the old tablet disintegrates. When the PVP K-30 gel is saturated and remains hydrated, the PVP K-30 dissolves. In this condition, the SSG particles swell, and the tablet disintegrates. The SSG particles swell depending on hydration rate and SSG concentration. When the hydration of SSG is slow, the old SSG particles swell, and the disintegration time of the tablets is long. When the concentration of SSG particles in the tablet is low, the SSG starts from the tablet's surface. The driving force against the particles begins from the surface towards the tablet core so that the tablet disintegrates gradually. The SSG*PVP K-30 reduces disintegration time because PVP K-30 is easily soluble and accelerates SSG's hydration, so the SSG particles swell immediately, and the tablet disintegrates.

The $4CH_2Cl$ is a new compound still being developed for dosage forms and has yet to be registered in regulations. The dissolution specification is at least 70% (Q) $4CH_2Cl$ is released within 45 min. All tablets in this experiment within 45 min released above 75% (Q + 5). The presence of soluble and semipolar PVP K-30 accelerates the hydration of $4CH_2Cl$ particles and dissolution (Kurakula and Rao, 2020). The materials that increase the dissolution the most, according to the quadratic model, are PVP K-30, SSG, and SSG*PVP K-30. The PVP K-30 dominates the dissolution of $4CH_2Cl$ because of its soluble and semipolar nature. The PVP K-30 accelerates the hydration of the tablet and its constituent particles so that the tablet disintegrates quickly, and the concentration of $4CH_2Cl$ is high in the dissolution medium. SSG's presence accelerates the separated tablet mass particles, including $4CH_2Cl$ particles. The interaction of $4CH_2Cl$ particles with the dissolution media causes $4CH_2Cl$ to dissolve. The combination of SSG*PVP K-30 increases the release of $4CH_2Cl$ because PVP K-30 accelerates the hydration of SSG particles so that the tablets are immediately crushed into granules and powders. The PVP K-30 dissolves in the dissolution media accelerates

hydration and dissolves $4CH_2Cl$ particles.

The $4CH_2Cl$ release kinetics model was determined by the highest Rsqr_adj, the lowest MSE_root, and the lowest AIC. Rsqr_adj describes the relationship between the dissolution time and the concentration of the dissolved. The MSE_root acts as the correlation analysis controller. The AIC determined the suitability of the release kinetics model equation (Gu et al., 2018; Mircioiu et al., 2019; Siswanto et al., 2015; Zhang et al., 2010).

The Ta tablets followed the kinetics of the Korsmeyer-Peppas model with the release of $4CH_2Cl$ by Fickian diffusion ($n = 0.18$). The high concentration of SSG causes $4CH_2Cl$ particles and other particles to be trapped in the swollen SSG particles. Diffusion of $4CH_2Cl$ through the pathway created by soluble PVP K-30 particles. The Tb and To tablets followed the Weibull kinetic model with a rapid release of $4CH_2Cl$. The PVP K-30, easily soluble in dissolution media, accelerates hydration and dissolution of $4CH_2Cl$ particles. The presence of SSG accelerates the disintegration of tablets into granules/powder so that the surface area for dissolving $4CH_2Cl$ particles is wider. The Tc tablets follow the first-order kinetics model with the release of $4CH_2Cl$ by diffusion through the porosity. Irregular PVP K-30 fragments cause a large amount of tablet or granule porosity. The diffusion mechanism of $4CH_2Cl$ particles occurs through the porosity of the granules.

The three experimental groups of analgesic activity showed significantly different activity responses ($P < 0.05$). The effectiveness of $4CH_2Cl$ pain inhibitors (Fig. 7) shows that the presence of excipients in To tablets does not interfere with the analgesic activity of $4CH_2Cl$.

5. Conclusion

SSG and PVP K-30 increased Carr index, Hausner ratio, hardness, friability, disintegration time, and drug release. The combination of SSG*PVP K-30 has the same effect, except that the disintegration time decreased. The optimum tablet formula is $4CH_2Cl$ (300 mg), Ne (75 mg), SSG (33.60 mg), PVP K-30 (22.40 mg), MCC (40 mg), and SDL (up to 800 mg). The tablet characteristics have Carr index (18.10), Hausner ratio (1.24), hardness (6.51 Kp), friability (0.54%), disintegration time (3.30 min), and drug release (9.30%). $4CH_2Cl$ tablets can be a candidate and choice for new analgesic drugs in the future.

Declaration of human and animal rights

The Research Ethics Commission of the Faculty of Veterinary Medicine, Gadjah Mada University Yogyakarta, Indonesia, stated that experiments using experimental animals (mice) had met the ethical requirements with a certificate No.001/EC-FKH/Ex./2022 dated January 14, 2022.

Availability of data and material

In addition to the tables and figures in the article, the research results present supporting data on the Supplementary Material: Tablet dosage calculation; the release of $4CH_2Cl$ from the tablets; statistical analysis of $4CH_2Cl$ tablets; the kinetics profile of the release of $4CH_2Cl$ from Ta, Tb, Tc, and To. tablets.

Credit author statement

Wuryanto Hadinugroho: Designed the experiments, performed the experiments, analyzed and interpreted the data, wrote the manuscript. Yudy Tjahjono, Kuncoro Foe, Senny Yesery Esar, Caroline Caroline, Maria Annabela Jessica, Hendy Wijaya: performed the experiments, analyzed, and interpreted the data.

Declaration of competing interest

On behalf of all authors, the corresponding author states that there is no conflict of interest.

Data availability

The authors do not have permission to share data.

Acknowledgment

Thanks to the Research and Community Service Institute of Widya Mandala Surabaya Catholic University, Surabaya, Indonesia, for supporting grants (5230/WM01/N/2021). Thanks to Angela Tiffany, Meidelin Ribka Abiati, Sherlilyta Stiara Dewi, and Khaterine Irene Phuk for their assistance during the experiment.

Appendix A. Supplementary data

Supplementary data to this article can be found online at https://doi.org/10.1016/j.crphar.2024.100200.

References

Aulton, M.E., Taylor, K.M.G., 2017. Aulton's Pharmaceutics the Design and Manufacture of Medicines, BMC Public Health. Churchill Livingstone Elsevier, New York.

Bertocchi, P., Antoniella, E., Valvo, L., Alimonti, S., Memoli, A., 2005. Diclofenac sodium multisource prolonged release tablets - a comparative study on the dissolution profiles. J. Pharm. Biomed. Anal. 37, 679–685. https://doi.org/10.1016/j.jpba.2004.11.041.

Caroline, Foe, K., Yesery Esar, S., Soewandi, A., Wihadmadyatami, H., Widharna, R.M., Tamayanti, W.D., Kasih, E., Tjahjono, Y., 2019a. Evaluation of analgesic and antiplatelet activity of 2-((3-(chloromethyl)benzoyl)oxy)benzoic acid. Prostag. Other Lipid Mediat. 145, 106364 https://doi.org/10.1016/j.prostaglandins.2019.106364.

Caroline, Nathania, Foe, K., Esar, S.Y., Jessica, M.A., 2019b. Characterization of pharmacokinetics of 2-((3-(chloromethyl)benzoyl)oxy) benzoic acid in rats by using hplc-dad method. Int. J. Appl. Pharm. 11, 279–283. https://doi.org/10.22159/ijap.2019v11i5.34536.

Chaerunisaa, A.Y., Sriwidodo, S., Abdassah, M., 2020. Microcrystalline cellulose as pharmaceutical excipient. Pharm. Formul. Des. - Recent Pract. https://doi.org/10.5772/intechopen.88092.

Coates, J., 2006. Interpretation of infrared spectra, A practical approach. Encycl. Anal. Chem. 10815–10837. https://doi.org/10.1002/9780470027318.a5606.

Craciun, A.M., Barhalescu, M.L., Agop, M., Ochiuz, L., 2019. Theoretical modeling of long-time drug release from nitrosalicyl-imine-chitosan hydrogels through multifractal logistic type laws. Comput. Math. Methods Med. 2009, 1–10. https://doi.org/10.1155/2019/4091464.

Dachriyanus, 2004. Spectroscopic Structural Analysis of Organic Compounds. Institute of Information and Communication Technology Development (LPTIK). Andalas University, Padang.

Flemming Jr., C., 2016. Quantitative Analysis of Acetylsalicylic Acid by Q- NMR (Quantitative-Nuclear Magnetic Resonance Spectroscopy). Theses.

Gu, Y., Wei, H.L., Balikhin, M.M., 2018. Nonlinear predictive model selection and model averaging using information criteria. Syst. Sci. Control Eng. 6, 319–328. https://doi.org/10.1080/21642583.2018.1496042.

Hadinugroho, W., Foe, K., Tjahjono, Y., Caroline, C., Yesery Esar, S., Wijaya, H., Annabella Jessica, M., 2022a. Tablet formulation of 2-((3-(chloromethyl)benzoyl) oxy)benzoic acid by linear and quadratic models. ACS Omega 7, 34045–34053. https://doi.org/10.1021/acsomega.2c03147.

Hadinugroho, W., Martodihardjo, S., Fudholi, A., Riyanto, S., 2022b. Preparation of citric acid-locust bean gum (CA-LBG) for the disintegrating agent of tablet dosage forms. J. Pharm. Innov. 17, 1160–1175. https://doi.org/10.1007/s12247-021-09591-0.

Juneja, P., Kaur, B., Odeku, O.A., Singh, I., 2014. Development of corn starch-neusilin UFL2 conjugate as tablet superdisintegrant: formulation and evaluation of fast disintegrating tablets. J. Drug Deliv. 2014, 1–13. https://doi.org/10.1155/2014/827035.

Kaleemullah, M., Jiyauddin, K., Thiban, E., Rasha, S., Al-Dhalli, S., Budiasih, S., Gamal, O.E., Fadli, A., Eddy, Y., 2017. Development and evaluation of Ketoprofen sustained release matrix tablet using Hibiscus rosa-sinensis leaves mucilage. Saudi Pharmaceut. J. 25, 770–779. https://doi.org/10.1016/j.jsps.2016.10.006.

Kupriyanova, G., Rafalskiy, V., Mershiev, I., Moiseeva, E., 2021. NMR spectroscopy reveals acetylsalicylic acid metabolites in the human urine for drug compliance monitoring. PLoS One 16, 1–12. https://doi.org/10.1371/journal.pone.0247102.

Kurakula, M., Rao, G.S.N.K., 2020. Pharmaceutical assessment of polyvinylpyrrolidone (PVP): as excipient from conventional to controlled delivery systems with a spotlight on COVID-19 inhibition. J. Drug Deliv. Sci. Technol. 60, 102046 https://doi.org/10.1016/j.jddst.2020.102046.

Lou, H., Liu, M., Wang, L., Mishra, S.R., Qu, W., Johnson, J., Brunson, E., Almoazen, H., 2013. Development of a mini-tablet of co-grinded prednisone-neusilin complex for pediatric use. AAPS PharmSciTech 14, 950–958. https://doi.org/10.1208/s12249-013-9981-x.

Markl, D., Zeitler, J.A., 2017. A review of disintegration mechanisms and measurement techniques. Pharm. Res. (N. Y.) 34, 890–917. https://doi.org/10.1007/s11095-017-2129-z.

Mircioiu, C., Voicu, V., Anuta, V., Tudose, A., Celia, C., Paolino, D., Fresta, M., Sandulovici, R., Mircioiu, I., 2019. Mathematical modeling of release kinetics from supramolecular drug delivery systems. Pharmaceutics 11, 1–18. https://doi.org/10.3390/pharmaceutics11030140.

Panotopoulos, G.P., Haidar, Z.S., 2018. Mathematical modeling for pharmacokinetic predictions from controlled drug release nano systems: a comparative parametric study. Biomed. Pharmacol. J. 11, 1801–1806. https://doi.org/10.13005/bpj/1552.

Sheskey, P.J., Walter, C.G., Cable, C.G., 2017. Handbook of Pharmaceutical Excipients, eighth ed. Pharmaceutical Press and American Pharmacists Association, London-Washington DC.

Shete, A., Salunkhe, A., Yadav, A., Sakhare, S., Doijad, R., 2019. Neusilin based liquisolid compacts of albendazole: design, development, characterization and in vitro anthelmintic activity. Marmara Pharm. J. 23, 441–456. https://doi.org/10.12991/jrp.2019.151.

Siswanto, A., Fudholi, A., Nugroho, A.K., Martono, S., 2015. In vitro release modeling of aspirin floating tablets using ddsolver. Indones. J. Pharm. 26, 94. https://doi.org/10.14499/indonesianjpharm26iss2pp94.

Sugiarno, F.D., 2016. 2-(4-chloromethyl)benzoyl)oxy)benzoate in male white rats (Rattus norvegicus). Theses.

Suhartati, T., 2017. Basic of UV-VIS spectrophotometry and mass spectromistry for structural determination of organic compounds. Anugrah Utama Raharja, Bandar Lampung.

Tamayanti, W.D., Widharna, R.M., Caroline, C., Soekarjo, B., 2016. Uji aktivitas analgesik asam 2-(3-(Klorometil)Benzoiloksi)Benzoat dan asam 2-(4-(Klorometil) Benzoiloksi)Benzoat pada tikus wistar jantan dengan metode plantar test. J. Pharm. Sci. Community 13, 15–22. https://doi.org/10.24071/jpsc.131125.

The United States Pharmacopeial Convention, 2018. Pharmacopeia 41-National Formulary 36. Twinbrook Parkway, Rockville.

Thoorens, G., Krier, F., Leclercq, B., Carlin, B., Evrard, B., 2014. Microcrystalline cellulose, a direct compression binder in a quality by design environment - a review. Int. J. Pharm. 473, 64–72. https://doi.org/10.1016/j.ijpharm.2014.06.055.

Tjahjono, Y., Caroline, Foe, K., Wijaya, H., Dewi, B.D.N., Karnati, S., Esar, S.Y., Karel, P., Partana, F.R., Henrikus, M.A., Wiyanto, C.A., Wilianto, Y.R., Hadinugroho, W., Nugraha, J., Nugrahaningsih, D.A.A., Kusindarta, D.L., Wihadmadyatami, H., 2024. 2-(3-(Chloromethyl)benzoyloxy)benzoic Acid reduces prostaglandin E-2 concentration, NOX2 and NFKB expression, ROS production, and COX-2 expression in lipopolysaccharide-induced mice. Prostag. Other Lipid Mediat. 174, 106866 https://doi.org/10.1016/j.prostaglandins.2024.106866.

Tjahjono, Y., Karnati, S., Foe, K., Anggara, E., Gunawan, Y.N., Wijaya, H., Steven, Suyono, H., Esar, S.Y., Hadinugroho, W., Wihadmadyatami, H., Ergun, S., Widharna, R.M., Caroline, 2021. Prostaglandins and Other Lipid Mediators Acid in LPS-Induced Rat Model 154. https://doi.org/10.1016/j.prostaglandins.2021.106549.

Wahab, A., Khan, G.M., Akhlaq, M., Khan, N.R., Hussain, A., Khan, M.F., Khan, H., 2011. Formulation and evaluation of controlled release matrices of ketoprofen and influence of different co-excipients on the release mechanism. Pharmazie 66, 677–683. https://doi.org/10.1691/ph.2011.1040.

Yasmin, R., Shoaib, M.H., Ahmed, F.R., Qazi, F., Ali, H., Zafar, F., 2020. Aceclofenac fast dispersible tablet formulations: effect of different concentration levels of Avicel PH102 on the compactional, mechanical and drug release characteristics. PLoS One 15, e0223201. https://doi.org/10.1371/journal.pone.0223201.

Zhang, Y., Huo, M., Zhou, J., Zou, A., Li, W., Yao, C., Xie, S., 2010. DDSolver: an add-in program for modeling and comparison of drug dissolution profiles. AAPS J. 12, 263–271. https://doi.org/10.1208/s12248-010-9185-1.

Zupančič-Božič, D., Vrečer, F., Kozjek, F., 1997. Optimization of diclofenac sodium dissolution from sustained release formulations using an artificial neural network. Eur. J. Pharmaceut. Sci. 5, 163–169. https://doi.org/10.1016/S0928-0987(97)00273-X.

Characterization of 2-((4-(chloromethyl)benzoyl)oxy)benzoate acid for analgesic tablet dosage form formulation

ORIGINALITY REPORT

3%	1%	3%	1%
SIMILARITY INDEX	INTERNET SOURCES	PUBLICATIONS	STUDENT PAPERS

PRIMARY SOURCES

1	Great Iruoghene Edo, Alice Njolke Mafe, Patrick Othuke Akpoghelie, O. Tubi Abiola et al. "Current Advances in the Therapeutic Potential of Scutellarin: Novel Applications, Mechanisms, and Future Challenges.", Phytomedicine Plus, 2025 Publication	1%
2	Caroline, Kuncoro Foe, Senny Yesery Esar, Ami Soewandi et al. "Evaluation of analgesic and antiplatelet activity of 2-((3-(chloromethyl)benzoyl)oxy)benzoic acid", Prostaglandins & Other Lipid Mediators, 2019 Publication	1%
3	Submitted to University of Nottingham Student Paper	1%
4	Sameer J. Nadaf, Pranav L. Savekar, Durgacharan A. Bhagwat, Komal V. Dagade, Shailendra S. Gurav. "Revolutionizing fast disintegrating tablets: Harnessing a dual approach with porous starch and sublimation technique", Heliyon, 2024 Publication	1%

Exclude quotes	On	Exclude matches	< 1%
Exclude bibliography	On		

Characterization of 2-((4-(chloromethyl)benzoyl)oxy)benzoate acid for analgesic tablet dosage form formulation

GRADEMARK REPORT

FINAL GRADE

/100

GENERAL COMMENTS

PAGE 1

PAGE 2

PAGE 3

PAGE 4

PAGE 5

PAGE 6

PAGE 7

PAGE 8

PAGE 9

PAGE 10